Impact Assessment of Assimilating NASA's RapidScat Surface Wind Retrievals in the NOAA Global Data Assimilation System

LING LIU

Atmospheric Environmental Research, Inc., College Park, Maryland

KEVIN GARRETT AND ERIC S. MADDY

Riverside Technology, Inc., College Park, Maryland

SID-AHMED BOUKABARA

NOAA/NESDIS/Center for Satellite Applications and Research, College Park, Maryland

(Manuscript received 9 May 2016, in final form 1 September 2017)

ABSTRACT

The National Aeronautics and Space Administration (NASA) RapidScat scatterometer on board the International Space Station (ISS) provides observations of surface winds that can be assimilated into numerical weather prediction (NWP) forecast models. In this study, the authors assess the data quality of the RapidScat Level 2B surface wind vector retrievals and the impact of those observations on the National Oceanic and Atmospheric Administration (NOAA) Global Forecast System (GFS). The RapidScat is found to provide quality measurements of surface wind speed and direction in nonprecipitating conditions and to provide observations that add both information and robustness to the global satellite observing system used in NWP models. The authors find that with an assumed uncertainty in wind speed of around 2 m s^{-1}, the RapidScat has neutral impact on the short-range forecast of surface wind vectors in the tropics but improves both the analysis and background field of surface wind vectors. However, the deployment of RapidScat on the ISS presents some challenges for use of these wind vector observations in operational NWP, including frequent maneuvers of the spacecraft that could alter instrument performance.

1. Introduction

Current numerical weather prediction (NWP) models assimilate near-surface wind speed vectors from both conventional and spaceborne satellite observations. Conventional sources over ocean are from a spatially coarse network of buoys and ships and offer observations at high temporal frequency. Observations from spaceborne low-Earth-orbiting (LEO) satellites provide much broader spatial coverage but may only observe the same location on Earth twice per day. Therefore, adding satellite sensors capable of deriving surface wind vectors to the current global satellite observing system would increase the density and temporal coverage provided to data assimilation systems.

Observations of sea surface wind speed and direction derived from space provide important information to NWP data assimilation about the location and intensity of baroclinic zones and cyclones and the strength of large-scale circulation patterns to improve initial conditions (e.g., the analysis) and subsequent forecasts. For example, Yu and McPherson (1984) demonstrated positive impact on Southern Hemisphere (SH) wind and height analyses from assimilating *Seasat* scatterometer vector winds. More recently, Fan et al. (2013) assimilated QuikSCAT ocean surface winds into the Weather Research and Forecasting (WRF) regional model using a 3DVar data assimilation system (WRF-DA). They found that assimilating QuikSCAT wind vectors could potentially improve the forecast of near–sea surface wind in the Chukchi and Beaufort Seas region. Chen (2007) compared the impact of assimilating Defense Meteorological Satellite Program (DMSP) Special Sensor Microwave Imager (SSM/I) and the QuikSCAT satellite surface winds data into the fifth-generation Pennsylvania State University–National Center for Atmospheric Research (PSU–NCAR) Mesoscale Model

Corresponding author: Ling Liu, ling.liu@noaa.gov

DOI: 10.1175/MWR-D-16-0179.1

(MM5; Grell et al. 1994) and its 3DVar data assimilation system, and found higher increments in wind analysis when QuikSCAT is assimilated, compared to assimilating SSM/I. Also, in the experiments assimilating QuikSCAT, the air–sea interaction process and the intensity of Hurricane Isidore were both enhanced, compared to experiments without assimilating QuikSCAT, indicating positive impact from QuikSCAT. Bi et al. (2011) assimilated and assessed the 50-km-resolution wind vector data of the Advanced Scatterometer (ASCAT) into the National Oceanic and Atmospheric Administration (NOAA) Global Data Assimilation System/Global Forecast System (GDAS/GFS). They found that by assimilating ASCAT, there is modest improvement (up to 40%) in the performance of GFS 24-h forecast of the wind field at midlatitudes.

In September 2014, the National Aeronautics and Space Administration (NASA) launched the RapidScat scatterometer as a follow-on to the QuikSCAT mission for continuity of surface wind vector observations over Earth. The RapidScat sensor is essentially identical to QuikSCAT (Chen 2007; Fan et al. 2013), with the primary difference being that it is deployed on the International Space Station (ISS) platform. Although the lower-orbiting altitude of ISS, compared to QuikSCAT, results in a narrower swath width of the RapidScat instrument, its deployment has added robustness to the global satellite observing system by providing complementary observations to other spaceborne scatterometers, including ASCAT, on board the Meteorological Operational (MetOp) platforms (Figa-Saldaña et al. 2002). The objective of this study is to assess the impact of assimilating RapidScat surface wind vector retrievals in the NOAA GDAS/GFS. Since the system already assimilates a large number of satellite observations, including surface wind, we investigate the additional benefits that can be obtained by assimilating RapidScat data. To realize these benefits, the proper quality control procedures that will lead to optimal analyses and forecasts are also discussed.

This study is outlined into five sections. Section 2 introduces the RapidScat sensor and the data to be assessed and assimilated. Section 3 shows the preassimilation RapidScat data quality assessment, including the description of the assessment approach and resulting quality control procedures. In section 4, we assess the impact of RapidScat on both the analysis and forecast. The conclusions of this study will be drawn in section 5.

2. RapidScat sensor and data description

a. ISS and RapidScat description

The ISS has been continually orbiting Earth since 1998. Because it is a manned spacecraft, the orbital characteristics are complicated due to safety procedures, docking procedures with other spacecraft, and the requirements of the various ongoing scientific research experiments. For example, the ISS orbits at altitudes varying between 375 and 435 km and has dynamic pitch, roll, and yaw of between 0° and 10°, less than 1°, and around −6°, respectively (Cooley 2013). These unique orbital characteristics pose a challenge for providing stable and well-calibrated Earth observations from onboard remote sensing instruments.

The RapidScat sensor, a rotating dual pencil-beam scatterometer, was installed on the ISS Columbus module in September 2014. The sensor uses a 13.4-GHz radar with a 0.75-m-diameter rotating dish antenna and a cross-track swath width on the order of 900 km for the inner beam and ~1100 km for the outer beam. RapidScat emits microwave signals toward Earth's surface in both horizontal (H-pol) and vertical polarization (V-pol) directions, with the incidence angles being within 44°–54° for the horizontal direction and 50°–60° in the vertical (Paget et al. 2016; NASA 2016). The ISS is on a prograde 51.6°-inclination, non-sun-synchronous orbit. Data coverage of RapidScat sensor is, therefore, restricted to the tropical and midlatitude regions (Rodriguez 2013). However, the sensor will observe all points at latitudes less than 50° at varying times of day over a 2-month repeat cycle. This feature allows almost a full coverage and a relatively accurate estimation of the semidiurnal and diurnal wind components observation from RapidScat data alone (Madsen and Long 2016; Rodriguez 2013; Paget et al. 2016).

b. RapidScat data description

In this study, RapidScat level 2B ocean surface wind vector retrievals provided by the NASA Jet Propulsion Laboratory (JPL) are assessed and assimilated. The level 2B wind vectors are binned on a 12.5-km wind vector cell (WVC) grid and processed using the level 2A sigma-0 dataset. The scatterometer winds have multiple ambiguities, meaning there are up to four wind solutions in each wind vector cell observed by RapidScat. These ambiguities are removed by constraining the spatial characteristics of the wind field, such as wind vector rotation (Fore et al. 2014). The ambiguity information is contained in the ambiguity quality control (QC) flag and can be removed by checking those flags in the RapidScat data.

As mentioned previously, the characterization of RapidScat data depends heavily on the stability of the ISS platform. Figure 1 shows the time series of RapidScat incidence angle (top) and wind speed bias (bottom) calculated against NOAA GFS forecasts for the year 2015. The incidence angle is shown for both the fore and aft views on the inner (H-pol) beam and outer (V-pol) beam. The wind speed bias is shown for both uncorrected (blue) and corrected (red) data, where the correction is performed for observations flagged as containing precipitation. The time

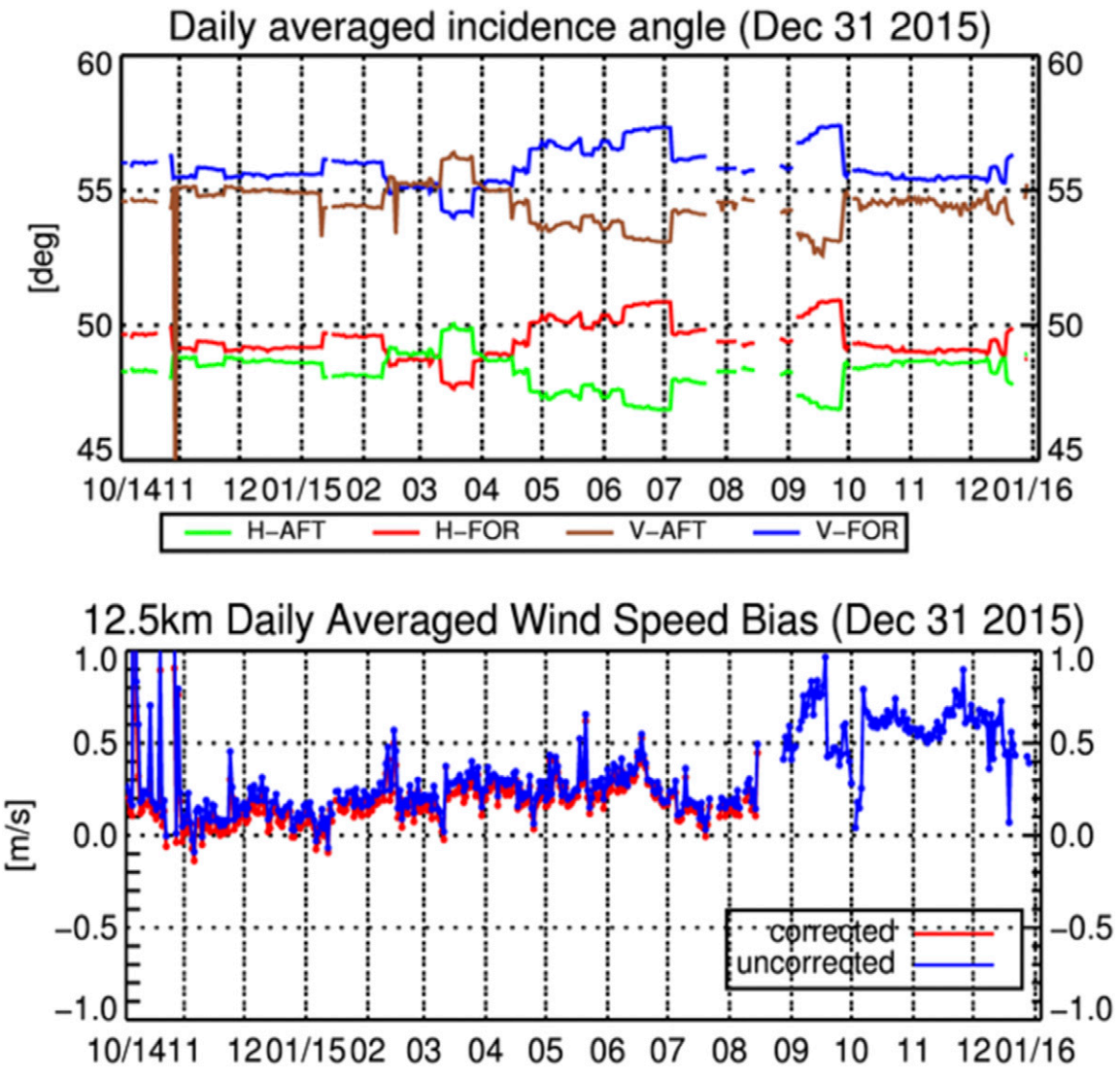

FIG. 1. Time series of (top) daily averaged incidence angle and (bottom) wind speed bias during 2015 (*x* axes) (http://manati.star.nesdis.noaa.gov/datasets/RSCATData.php); H-FOR and H-AFT are the horizontally polarized fore and aft views, respectively, and V-FOR and V-AFT are the vertically polarized fore and aft views, respectively. Note the fore and aft views are out of phase. The wind speed bias is the difference between the retrieved wind speed and the modeled (GFS) wind speed.

series of the incidence angle shows both drift and abrupt changes due to changes in the ISS orbit and orientation. The corresponding wind speed bias over the same period correlates well with the incidence angle, and it also displays abrupt spikes in the bias at periodic intervals due to changes in spacecraft orientation before it is recalibrated. In addition to the instability caused by the ISS maneuvers, the signal-to-noise ratio (SNR) of the RapidScat receiver dropped by 10 dB beginning in August 2015 (so-called low-SNR mode) due to an instrument anomaly. The low-SNR mode prevents accurate measure of brightness temperatures used to determine RapidScat precipitation flags and subsequent correction algorithms from performing optimally (NASA 2015). It should also be noted that the increase in the wind speed bias for uncorrected wind speeds remains greater than $0.5\,\mathrm{m\,s^{-1}}$ since low-SNR mode was activated. RapidScat data monitoring is done continuously in near–real time at the NOAA Center for Satellite Applications and Research (STAR) and can be accessed from http://manati.star.nesdis.noaa.gov.

3. RapidScat data quality assessment

a. Assessment method

The scope of this work is to assimilate RapidScat surface wind vector retrievals in the NOAA GDAS/GFS and to assess the impact on both the analysis and forecast performance. In fact, the GDAS/GFS currently

assimilates a large number of surface wind vector observations, including those from ASCAT on both *MetOp-A* and *MetOp-B* satellites, and also from radiosonde and surface stations. Therefore, we aim to assess the additional benefits of assimilating the RapidScat surface wind vectors on top of the current global observing system. To perform both the assimilation and assessment, it is important to properly characterize the RapidScat data quality and develop appropriate quality control procedures, as well as identify biases and define the observation errors, which determine how well the assimilation fits the observations. To illustrate the RapidScat data quality, we performed a preassimilation assessment for a single day of data from 15 June 2015. The surface wind speed and wind direction derived from RapidScat are compared to collocated ECMWF surface wind vectors. The selection of the sample day is due to the stability of the RapidScat data during that time period and before the switch to low-SNR mode.

Since the RapidScat scatterometer operates at a Ku-band radar wavelength (13.5 GHz), the atmosphere is not transparent, and wind speed signal from the surface can be contaminated by hydrometeors and near-surface precipitation. Moderate-to-heavy rain may cause spurious wind speed retrievals with errors up to 15–20 m s^{-1} (Draper and Long 2002; Jones and Zec 1996). To detect these contaminated observations, a rain flag based on simulated brightness temperatures at 37 GHz is checked from the level 2B data. Therefore, the first step in the quality control of the data is to discard points flagged as raining and only assess nonprecipitation-affected observations.

Figure 2 shows the difference between RapidScat and ECMWF wind direction versus the ECMWF wind speed for 15 June 2015 after filtering out precipitating observations. The mean bias is illustrated by the solid red line, while the standard deviation is the dashed red line. The wind direction standard deviation shows a dramatic increase for wind speeds less than 5 m s^{-1}, while the bias of wind direction remains close to zero for wind speeds less than 20 m s^{-1}. The wind vectors associated with large wind direction differences are due to the increased variability at low wind speeds in both the model estimation and in the observations (Gonzales and Long 1999). Fore et al. (2014) found that the ambiguity removal was not performed as successfully for wind vectors with wind speed less than 3 m s^{-1}. Therefore, the second step in quality control is to establish a low wind speed cutoff and remove observations less than 5 m s^{-1} due to the larger uncertainties in wind direction. The impact of this filter will be shown in the following section.

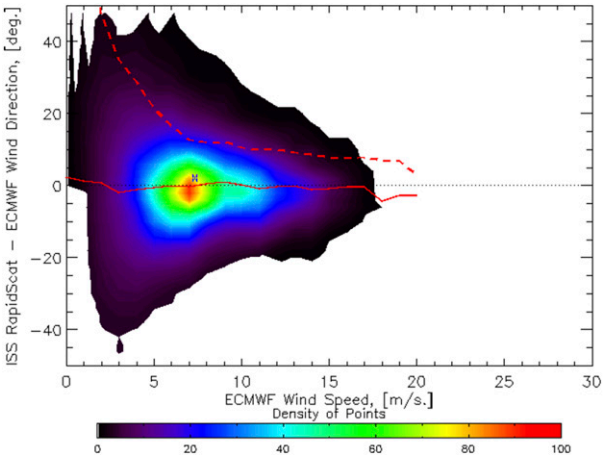

FIG. 2. Preassimilation result: difference between RapidScat and ECMWF wind direction (°), stratified against ECMWF wind speed (m s^{-1}) for 15 Jun 2015. Standard deviation is indicated by dashed red line and bias is solid red line. Color of contour stands for density of points; see color bar.

b. *Overall data quality assessment*

The overall preassimilation data quality assessment of RapidScat surface wind vector observations on 15 June 2015 is illustrated by Fig. 3. Figures 3a–c show maps of the difference between RapidScat and ECMWF wind speed before and after the rain and QC filters are applied, respectively. Figures 3d–f show maps of the difference between RapidScat and ECMWF wind direction, before and after the rain and QC filters are applied, respectively. The maps before QC show large differences in both speed and direction, qualitatively aligned with the intertropical convergence zone (ITCZ), as well as the midlatitude storm tracks in both the Northern Hemisphere (NH) and SH, indicating areas where the scatterometer signal is likely affected by moderate-to-heavy precipitation. However, most of the wind speed differences globally are well below 3 m s^{-1}, and wind direction differences are below 45°. After applying the rain and QC filters, many of the high wind speed and direction differences between RapidScat and ECMWF are removed.

Table 1 shows the standard deviation of the difference between RapidScat and ECMWF wind speed and direction for 15 June 2015, corresponding to the unfiltered and filtered maps in Fig. 3. The statistics show the count and standard deviation of wind speed and direction for unfiltered observations, after applying the rain flag check and after applying both the rain flag check and the 5 m s^{-1} low wind speed cutoff. After applying the rain flag check, the wind speed standard deviation is reduced from 2.3 to 1.9 m s^{-1}, while the wind direction standard deviation is reduced from 25.6° to only 25°. The main impact on directional errors is by removing the low wind speeds below 5 m s^{-1}, which reduces the standard deviation to 19.3°. In this case, as expected, the wind speed error increases slightly to 2 m s^{-1} since all remaining points [number of

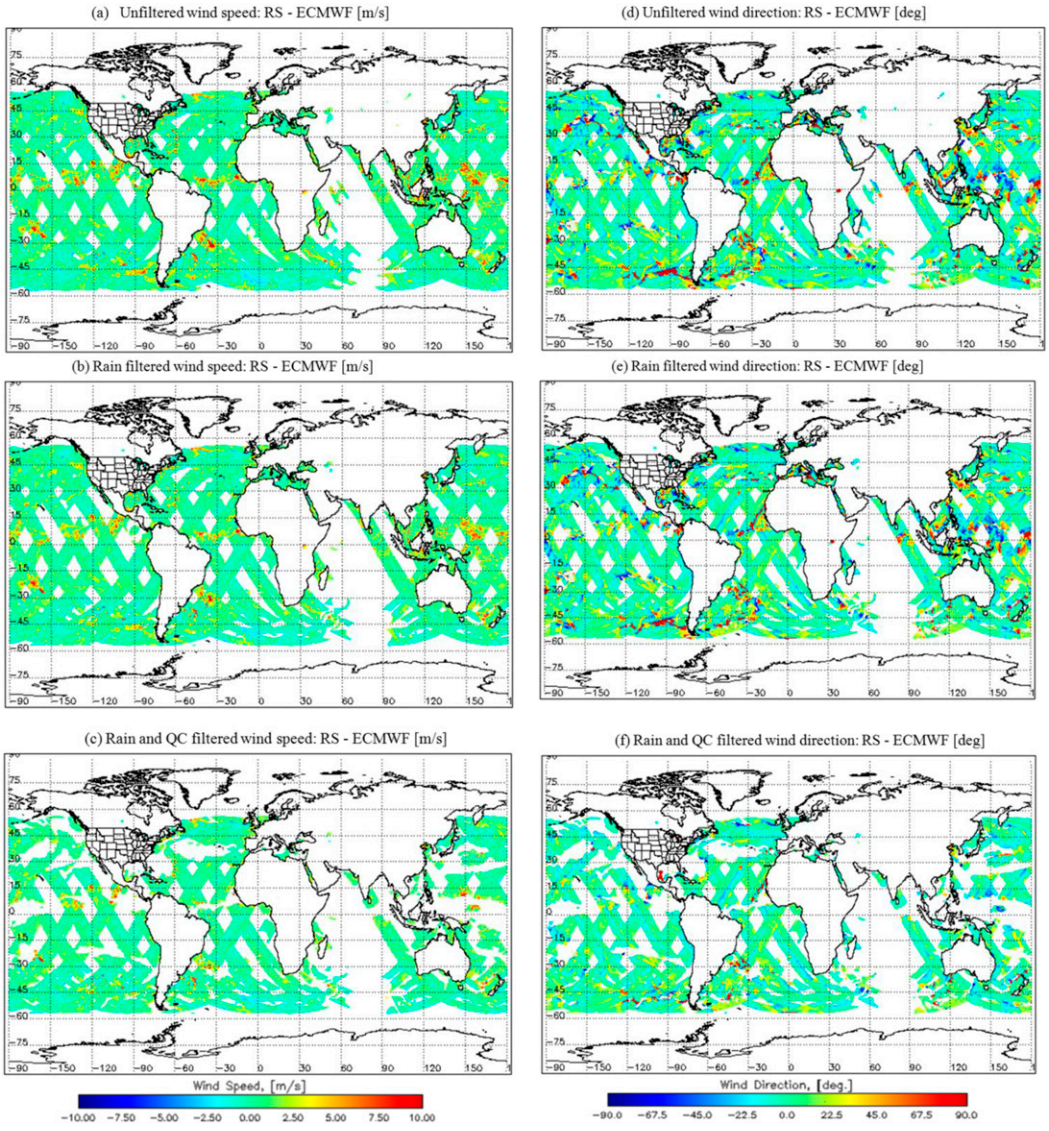

FIG. 3. Preassimilation result: maps illustrating the difference between RapidScat and ECMWF wind speed for (a) unfiltered, (b) after applying rain flag filter, and (c) after applying rain flag and low wind speed ($<5\,m\,s^{-1}$) filter. (d)–(f) As in (a)–(c), but for wind direction.

points after applying the $5\,m\,s^{-1}$ filter reduced from 2.1 to 1.3 million (M)] have wind speeds equal to or larger than $5\,m\,s^{-1}$. The preassimilation data quality assessment points to an overall error (standard deviation) of approximately $2\,m\,s^{-1}$ for RapidScat observations passing quality control, which will be prescribed as the required observation error in the data assimilation system (section 4).

4. Analysis and forecast impact assessment

a. Model description

The data assimilation system applied here is the hybrid 3DVAR–ensemble Kalman filter (EnKF) method employed in the Gridpoint Statistical Interpolation analysis system (GSI) (Wang et al. 2013). The GSI analysis, along with the 80 ensemble analyses and forecast members used to generate the ensemble portion of the background error covariance, is run at the T254L64 resolution (~50 km horizontal resolution, 64 vertical layers). The full GFS forecast (0–168 h) is run at the T574 resolution (~30 km horizontal resolution) and uses the semi-Lagrangian dynamics scheme (McClung 2014). The GDAS is cycled for all four synoptic times at 0000, 0600, 1200, and 1800 UTC, while the GFS 168-h forecast is only run at the 0000 UTC cycle, which is used to assess the impact on medium-range forecast skill. This is due to constraints on computing

TABLE 1. Preassimilation: standard deviation of RapidScat wind speed and wind direction vs ECMWF on 15 Jun 2015 unfiltered observations, after applying the rain flag filter and after applying the rain flag filter and removing wind speeds less than 5 m s^{-1}.

	Unfiltered	Rain flag	Rain flag + 5 m s^{-1} cutoff
Count (M)	2.1	1.7	1.3
Speed (m s^{-1})	2.3	1.9	2.0
Direction (°)	25.6	25.0	19.3

resources that are not available to run the full GFS forecast at all four standard synoptic times.

The GSI is the unmodified version from the January 2015 operational implementation, with the exception of adding capability to assimilate RapidScat. This includes the capabilities to assimilate all the various satellite radiance datasets, atmospheric motion vectors (AMVs), GPS radio occultation (GPSRO), conventional observations, and the QC mechanisms implemented for those data. It also includes the specifications used to assimilate the various satellite and conventional datasets, including observation error specification for each observation type and radiance bias correction schemes. The assimilation parameters are optimized and applied in operational implementation. Since GSI only assimilates the U and V components of wind vector, RapidScat wind speed and wind direction have been converted into control variable U and V components for ingest into the GSI through meteorological wind direction convention:

$$U = \text{wspd} \times \sin(\text{wdir}),$$
$$V = \text{wspd} \times \cos(\text{wdir}),$$

where wspd is the wind speed, and wdir is the wind direction. The GSI includes inner and outer loops, with the inner loop driving the minimization of the cost function and the outer loop producing the innovations and analysis increment.

Two experiments were performed to test the impact of assimilating RapidScat observations on top of the current global observation system: the control run (CNTRL), which uses conventional and satellite observations currently assimilated in the January 2015 operational implementation of GDAS, and the experiment (EXRS), where RapidScat data are assimilated in addition to the observations assimilated in CNTRL. The experiments were run for 2 months between 1 June and 31 July 2015, while the assessment period covers 15 June to 31 July 2015 to allow for a 15-day spinup period, since the initial conditions data were taken from the operational run at NOAA, and to allow for the adaptation of the background fields to the RapidScat data.

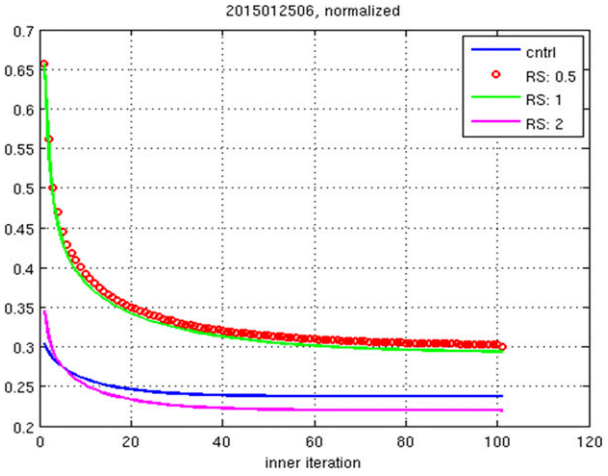

FIG. 4. Postassimilation results: normalized cost function for the CNTRL run without assimilating RapidScat (blue) and with assimilation of RapidScat for various observation errors, including 0.5 (red), 1 (green), and 2 m s^{-1} (magenta) derived from 1-month experiment running between 15 Jun and 15 Jul 2015.

b. *Postassimilation data assessment*

Prior to running the full experiment, cycles were run to verify the QC procedures, as well as to optimize the specification of the observation error used in the GSI. Figure 4 shows the normalized cost function for one GDAS cycle for CNTRL, as well as for EXRS, with observation errors of 0.5, 1, and 2 m s^{-1} specified for RapidScat versus the iteration number of the inner GSI loop. The normalization of the cost function is done by dividing the penalty by the number of observations assimilated. Using the prescribed observation error identical to the error calculated in the preassimilation data quality assessment of 2 m s^{-1} (RS: 2) shows a similar penalty to the CNTRL run. Though the penalty is higher at iteration zero, the cost function converges almost as quickly as CNTRL (after ~50 iterations). For more aggressive observation errors of 0.5 and 1.0 m s^{-1}, it is clear that the overall penalty increases drastically and that the gradient of the cost function (slope of the green and red curves) never becomes zero, even after 100 iterations (does not converge). Although there may be potential to reduce the observation errors slightly, based on the preassimilation data quality assessment, we maintain the 2 m s^{-1} observation error defined for the full experiment.

Figure 5 shows the scatterplots of the observed RapidScat surface wind speed and direction versus the background for four GDAS cycles (covering 1 day of observations). Figures 5a and 5c show the wind speed and direction comparison before the QC is applied, respectively. Figures 5b and 5d show the same

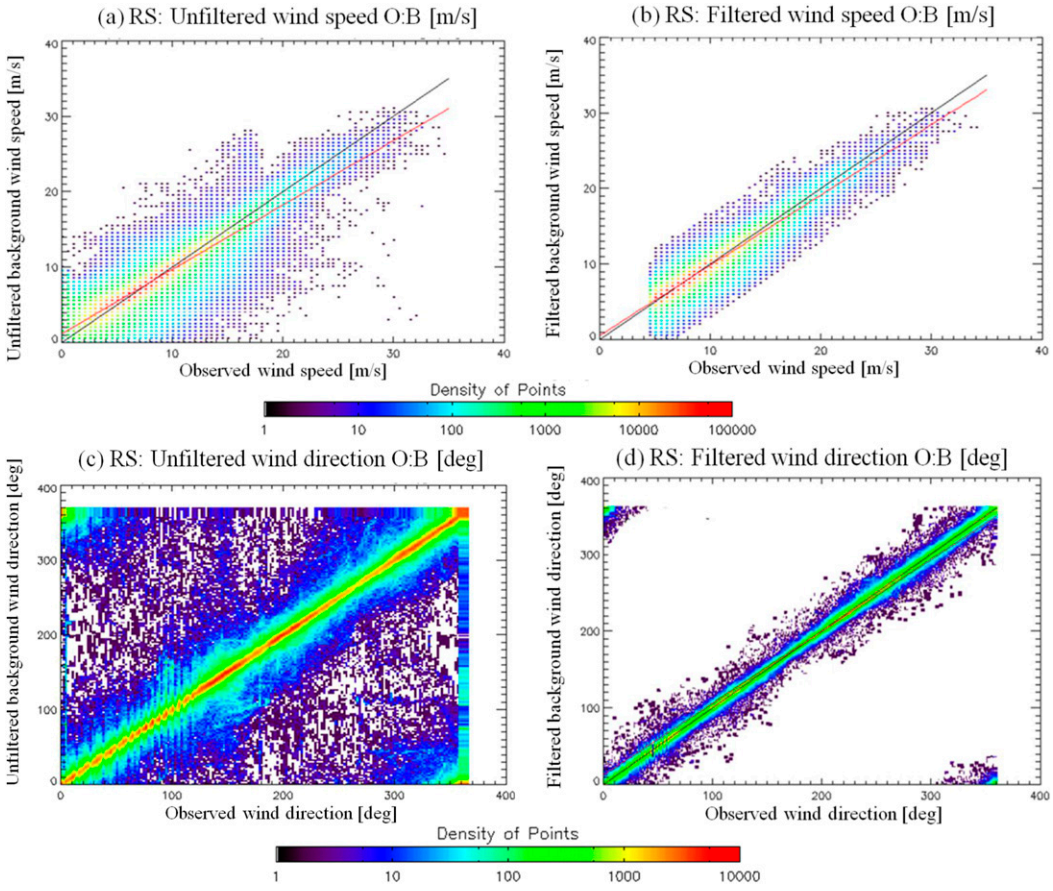

FIG. 5. Scatterplots of the observed RapidScat surface wind speed and direction vs the background wind speed and direction from GDAS for (a),(c) raw (unfiltered) data and (b),(d) filtered data after applying QC on the observations for June 2015. The black lines represent the one-to-one relationship. The red lines represent the linear fit of the scatterplot.

comparison but after the QC is applied to the RapidScat data. These comparisons show the effectiveness of the QC procedures that remove the outliers in both Figs. 5a and 5c. It should be noted that the points remaining in Fig. 5d close to 360° represent small directional differences between RapidScat and the background: for example, 0° and 360° can be considered the same direction.

TABLE 2. Postassimilation: standard deviation of RapidScat surface wind speed and direction vs the GDAS background ($O - B$) and analysis ($O - A$) for 15–16 Jun 2015. Statistics are shown for both unfiltered (no QC applied) and filtered (with QC applied) data.

	$O - B$ (unfiltered)	$O - B$ (filtered)	$O - A$ (unfiltered)	$O - A$ (filtered)
Count (M)	2.5	1.7	2.5	1.6
Speed ($m\,s^{-1}$)	1.7	1.4	1.5	1.2
Direction (°)	24.2	16.9	20.0	13.6

The summary statistics of RapidScat observed minus the GDAS background ($O - B$) before (unfiltered) and after QC (filtered) are shown in Table 2 for both wind speed and wind direction. The behavior of $O - B$ after applying QC is similar to that shown in the preassimilation assessment when the comparison of RapidScat to ECMWF analysis was performed: both impacts show a large reduction in standard deviation for wind speed and direction. It should be noted that the magnitude of the errors is smaller when

TABLE 3. Post assimilation: standard deviation of ASCAT wind speed and direction $O - B$ percent change with and without RapidScat assimilated vs the background, for 15-day GDAS cycles after 2-week spinup.

	CNTRL	EXRS	Change (%)
Count	852 208	852 208	0%
Speed ($m\,s^{-1}$)	1.22	1.21	1.0%
Direction (°)	24.2	23.9	1.1%

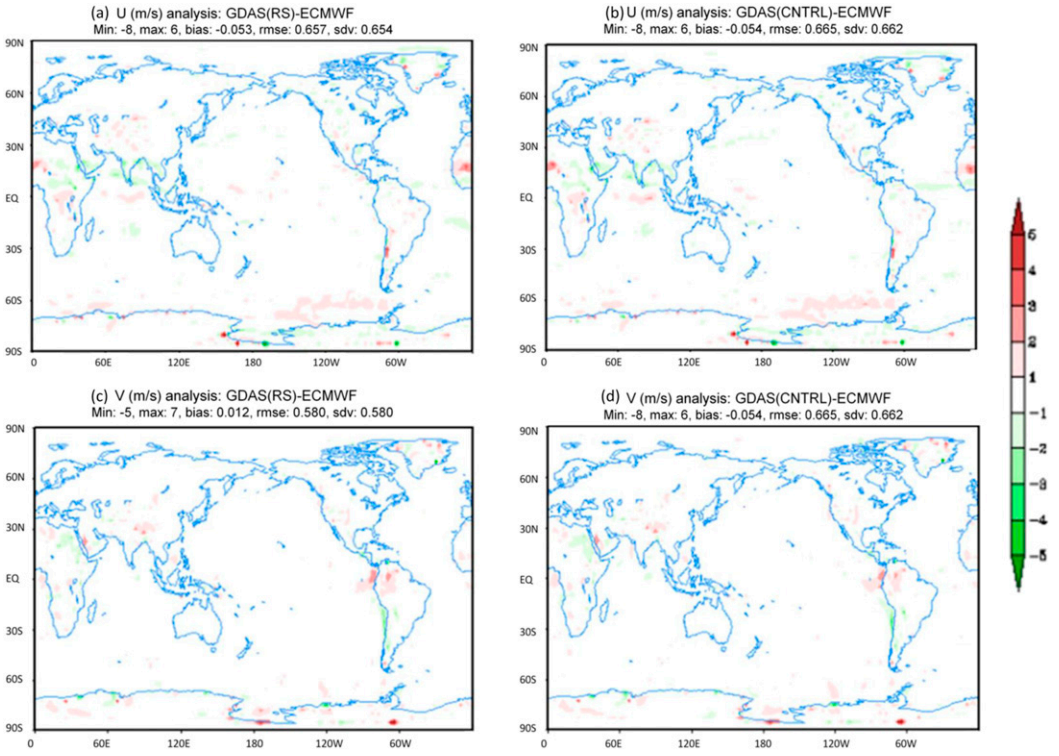

FIG. 6. Postassimilation results: map of the mean difference between GDAS analyses and ECMWF analyses at 850 hPa for (top) U- and (bottom) V-wind vector components when (a),(c) RapidScat is assimilated and (b),(d) without RapidScat assimilated. Statistics are derived from 1 month of data between 15 Jun and 15 Jul 2015.

compared to the GDAS background relative to the ECMWF analysis. This is likely due to the adjustment of the background field from the inclusion of RapidScat observations, which are not assimilated operationally in the ECMWF analysis used in the preassimilation assessment. Table 2 also shows the summary of statistics of RapidScat observed minus the analysis ($O - A$) before and after quality control is applied. The assimilation of RapidScat observations further reduces the standard deviation of wind speed from 1.4 to 1.2 $\mathrm{m\,s^{-1}}$ and wind direction from 16.9° to 13.6°, showing a fit to the RapidScat observations by the analysis well below the prescribed observation error of 2 $\mathrm{m\,s^{-1}}$.

Adding RapidScat observations on top of the current global observing system shows a small positive impact

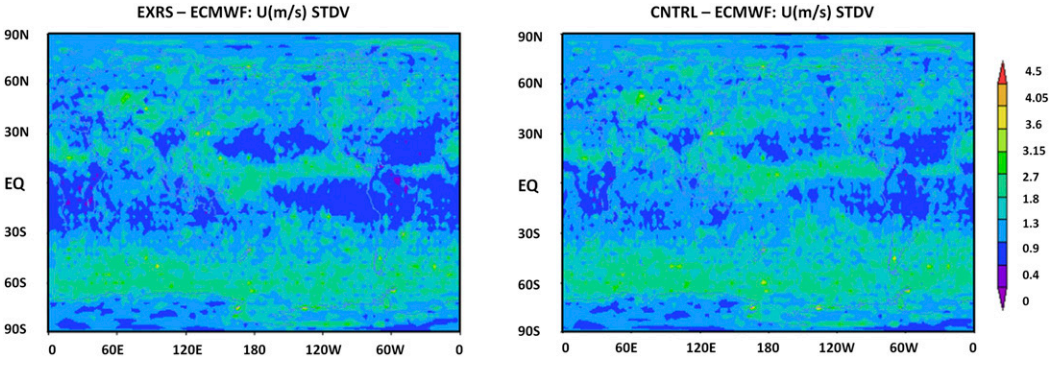

FIG. 7. Standard deviation of GDAS-ECMWF for the U component of the wind vector at 1000 hPa between 15 Jun and 15 Jul 2015. (left) Standard deviation of the U difference between the RapidScat experiment and ECMWF. (right) Standard deviation of the U difference between the CNTRL experiment and ECMWF.

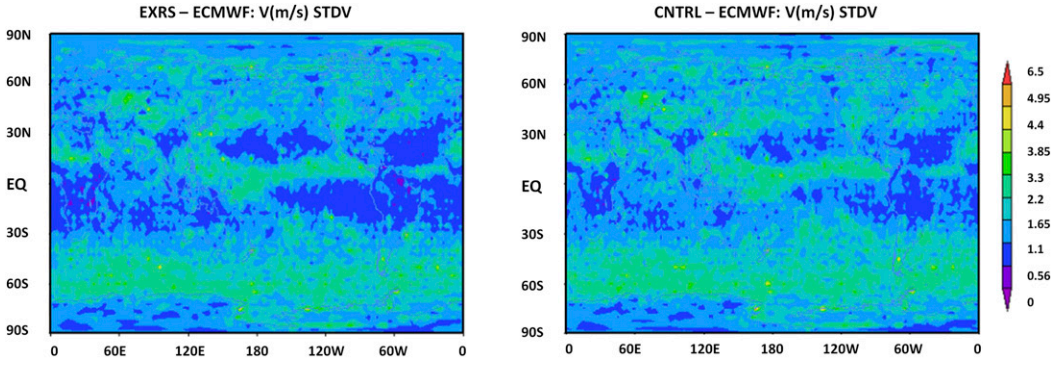

FIG. 8. Standard deviation of GDAS-ECMWF for the *V* component of the wind vector at 1000 hPa between 15 Jun and 29 Jul 2015. (left) Standard deviation of the *V* difference between the RapidScat experiment and ECMWF. (right) Standard deviation of the *V* difference between the CNTRL experiment and ECMWF.

on the assimilation of ASCAT data as well. Table 3 shows the ASCAT $O - B$ standard deviation when RapidScat is not assimilated (CNTRL) and when RapidScat is assimilated (EXRS) for 1 month of GDAS analysis cycles. For ASCAT, the wind speed $O - B$ standard deviation is slightly reduced from 1.22 to 1.21 m s^{-1}, while the direction standard deviation is reduced from 24.2° to 23.9° when RapidScat data are assimilated. This improvement demonstrates that RapidScat is adding information to the system by improving the background field wind vectors.

c. *Analysis impact assessment*

The GDAS analysis impacts from the assimilation of RapidScat wind vectors are assessed between 15 June and 31 July 2015. Figure 6 shows the mean bias between GDAS analyses and ECMWF for both *U* and *V* components of the 850-hPa wind vector. The comparison indicates up to 0.5% improvement with RapidScat surface wind vectors assimilated, mainly illustrated in removal of bias over the tropical Atlantic and southern Pacific Ocean areas. Figure 7 shows that the standard deviation between GDAS and ECMWF for the 1000-hPa *U*-wind component was improved over the tropics and subtropics after RapidScat was assimilated. This is demonstrated by the relatively larger areal coverage of dark blue shading. The 1000-hPa *V* component (Fig. 8) also shows improvement in the standard deviation using ECMWF as a reference, qualitatively similar to Fig. 7.

Table 4 provides a summary of the impact on the *U* and *V* analysis at 1000, 850, 500, and 200 hPa using ECMWF analysis as reference. There is similar impact on the improvement of standard deviation of *U* and *V* winds for 850, 500, and 200 hPa to what was shown for 1000 hPa in Figs. 7 and 8, showing that the assimilation of the RapidScat wind vector is having a small positive impact on the lower- and upper-level tropical and subtropical wind analyses.

d. *Forecast impact assessment*

An assessment of the impact on the GFS forecast from assimilating RapidScat observations was also performed for the period 15 June–31 July 2015, verified against the "self" analysis (i.e., the CNTRL is verified using the CNTRL analysis without assimilating RapidScat in GDAS, and EXRS is verified using the EXRS analysis including assimilation of RapidScat in GDAS). Figure 9 shows the forecast wind speed RMSE as a function of forecast hour in the tropics at 850 and 200 hPa. The RMSE for the CNTRL is shown in black, while the RMSE for EXRS is shown in red. The bottom panel of each plot shows the difference in RMSE with respect to the CNTRL experiment. Differences outside the red boxes are significant beyond the 95% confidence

TABLE 4. *U*- and *V*-wind vector components standard deviation (m s^{-1}) at 1000, 850, 500, and 200 hPa with and without the assimilation of RapidScat, compared to ECMWF analysis between 15 Jun and 31 Jul 2015.

Level (hPa)	*U* (EXRS) (m s^{-1})	*U* (CNTRL) (m s^{-1})	*V* (EXRS) (m s^{-1})	*V* (CNTRL) (m s^{-1})
1000	0.604	0.607	0.580	0.582
850	0.654	0.662	0.579	0.588
500	0.515	0.522	0.459	0.467
200	0.507	0.505	0.446	0.447

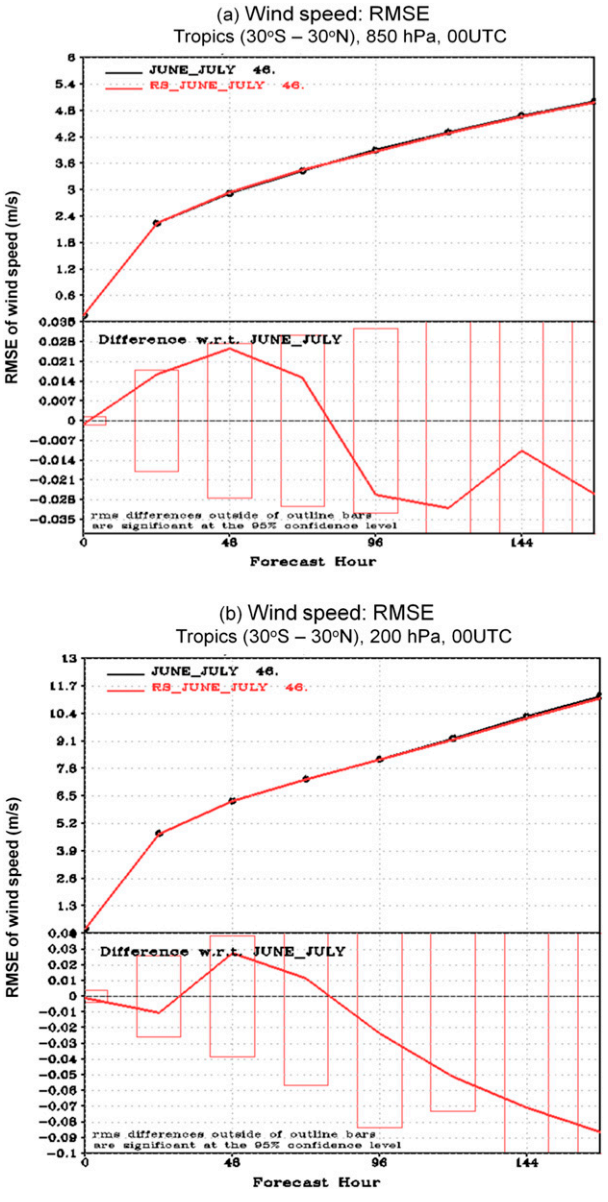

FIG. 9. GFS forecast of wind speed RMSE ($m\,s^{-1}$) as a function of forecast hour over the tropics at (a) 850 and (b) 200 hPa verified against the "self" analysis between 15 Jun and 31 Jul 2015 for the CNTRL (black) and EXRS (red) experiments. Bottom panels show the RMSE difference of EXRS with respect to CNTRL. Red boxes at each forecast hour represent the 95% significance interval.

interval. The impact on the tropical wind RMSE is neutral when assimilating RapidScat with some small increases or decreases at the various forecast hours, but not beyond the level of statistical significance, even near the surface at 850 hPa, where we expect RapidScat observations to have the most impact.

To summarize the impact assessment on wind forecasts verified against self-analyses, Table 5 lists the wind speed RMSE for day 1 and day 3 at 850 and 200 hPa for the tropics, NH, and SH. Overall, the impact for wind speed is relatively small and could be considered neutral. The day 1 RMSE is reduced when RapidScat is assimilated for 200 hPa over the tropics and NH, but it is increased over the tropics at 850 hPa and neutral elsewhere, but not beyond the 95% significance level (shown in Fig. 9 for the tropics). At day 3, the RMSE is the same or slightly higher for EXRS, compared with the CNTRL over most regions, except for 200 hPa in the NH, which is slightly reduced. As with the day 1 RMSE scores, the impact is not significant.

Further assessment of the wind forecast was performed by verifying against radiosonde observations. Figure 10 shows the vertical profile of wind speed bias and RMSE for the 24- and 48-h CNTRL and EXRS forecasts. The results show that there is no impact on wind forecasts when RapidScat observations are assimilated, as the bias and RMSE profiles are identical between the experiments at both forecast lead times. It should be noted that the radiosondes are assimilated in the GDAS/GFS and are highly weighted, so it is difficult to obtain better fits of the short-range forecast fields when adding new satellite observations.

Figure 11 shows the 500-hPa height anomaly correlation (AC) for CNTRL and EXRS as a function of forecast hour for both the NH and SH. Although the RapidScat observations are not directly sensitive to geopotential height or related parameters, the 500-hPa AC is a standard metric of medium-range predictability. While the assimilation of RapidScat brings very small impact on the NH geopotential height, it does have weak positive impact on the SH geopotential height but is not statistically significant. This could be explained by the fact that the SH has much less dense coverage of conventional observations than the NH and relies more on observations from satellites. The difference between the quantities of conventional data assimilated in each hemisphere is the main reason why assimilating RapidScat has a larger impact in the Southern Hemisphere.

e. *Discussion of RapidScat impacts*

In general, the improvement of adding RapidScat is limited because the assimilation experiments were performed on top of the current global data assimilation system, which also assimilates surface wind observations from scatterometers like ASCAT and in situ measurements from radiosonde, surface stations, and ocean buoys. Although there is an improvement to the GDAS analysis U and V wind vectors after assimilating RapidScat, it is difficult for such small impacts to propagate into medium-range forecasts, where modeling errors dominate with increasing forecast lead time. As shown

TABLE 5. Summary of RMSE of 850- and 200-hPa wind speed on day 1 and day 3 forecasts for NH, SH, and tropics (TRO) for experiment run between 15 Jun and 31 Jul 2015.

	NH: CNTRL	NH: EXRS	TRO: CNTRL	TRO: EXRS	SH: CNTRL	SH: EXRS
Day 1 RMSE						
850-hPa wind speed ($m\,s^{-1}$)	2.70	2.70	2.64	2.90	3.05	3.05
200-hPa wind speed ($m\,s^{-1}$)	3.83	3.83	4.92	4.91	3.55	3.54
Day 3 RMSE						
850-hPa wind speed ($m\,s^{-1}$)	4.36	4.39	3.55	3.56	5.82	5.83
200-hPa wind speed ($m\,s^{-1}$)	7.32	7.32	7.26	7.27	6.94	6.93

in section 4b and Fig. 4, the cost function with a prescribed RapidScat observation error of $2\,m\,s^{-1}$ does not contribute to more penalty in the DA system.

Although the primary objective of this work was to assess the impact of assimilating RapidScat when added to the current operationally assimilated global observing system, we performed a second set of experiments where all satellite observations were not assimilated in both the control (CNTRL_nosat) and with RapidScat (EXRS_nosat) experiments. This is both to confirm the successful implementation of RapidScat data assimilation and to quantify its impact without any redundant satellite observations, which could serve to minimize RapidScat's apparent contribution to NWP.

The experiments were performed between 1 June and 10 July 2015, with the period between 1 and 10 June as the spinup period and not included in the performance assessment. CNTRL_nosat assimilates conventional data only, including SST, temperature, humidity, and wind (U and V at all levels) retrieved from radiosonde, surface marine, and land observations with reported pressure, as well as splash-level dropsonde over ocean. Also assimilated are the aircraft and dropsonde temperature, pressure, and moisture (U and V at all levels), as well as wind profiler (U and V at all levels) and buoy data (surface wind). EXRS_nosat assimilates the above conventional data plus RapidScat surface wind. All other satellite data in both the CNTRL_nosat and

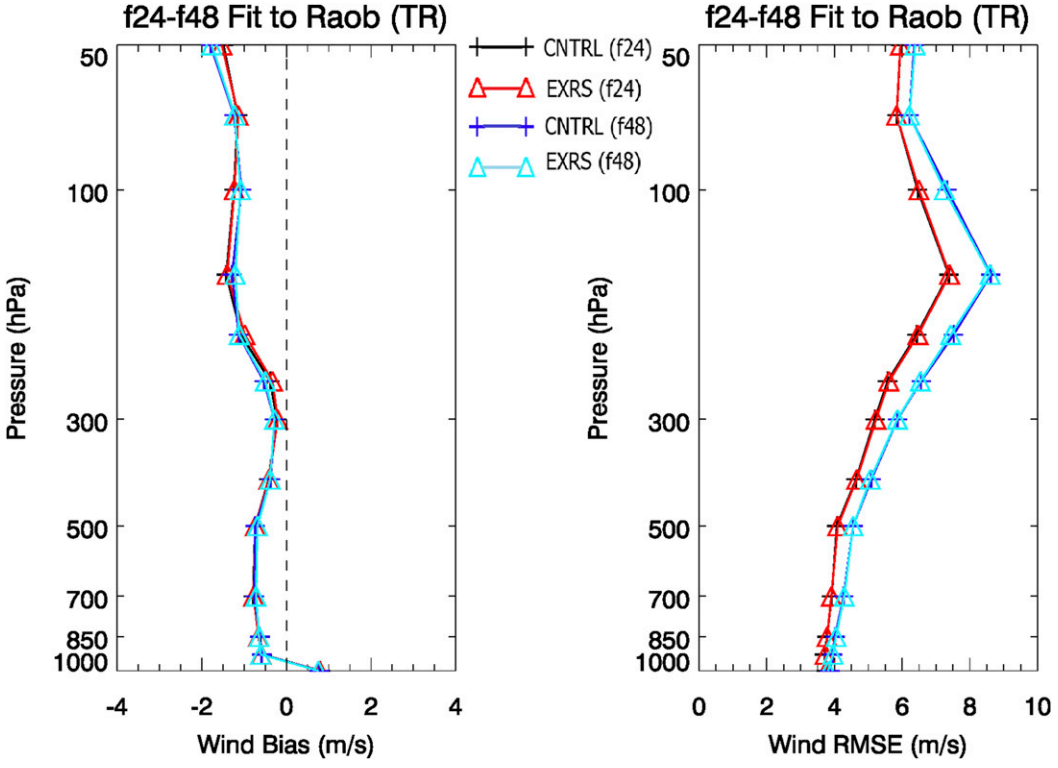

FIG. 10. (left) Wind speed bias and (right) RMSE for the 24- and 48-h CNTRL and EXRS experiment forecasts verified against tropical radiosonde.

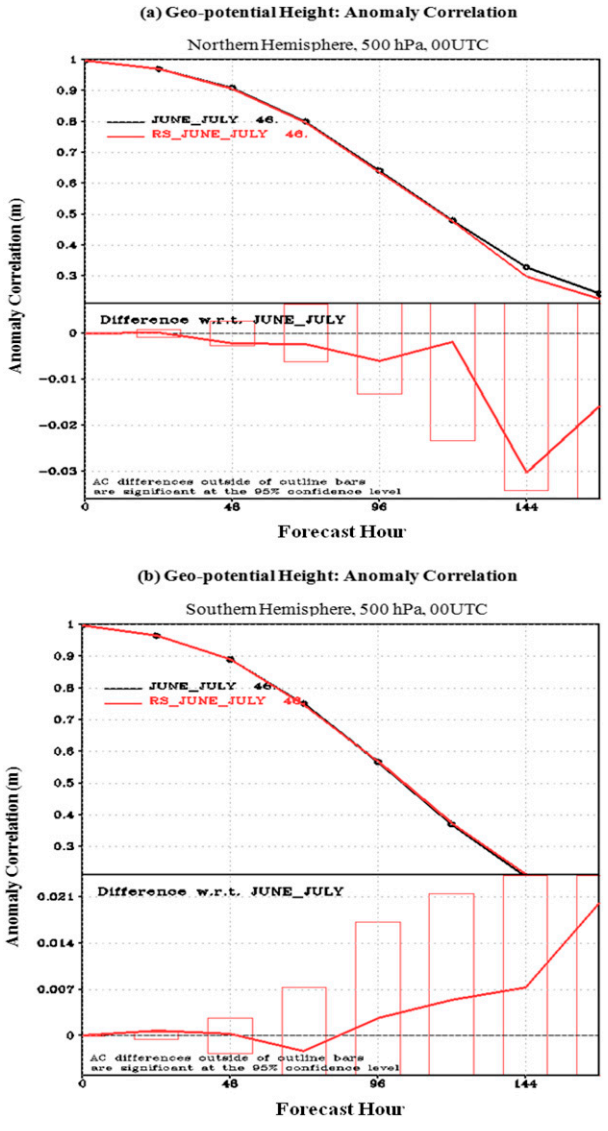

FIG. 11. GFS forecast of geopotential height AC as a function of forecast hour for (a) NH and (b) SH verified against the "self" analysis between 15 Jun and 31 Jul 2015 for the CNTRL (black) and EXRS (red) experiments. Bottom panels show the RMSE difference of EXRS with respect to CNTRL. Red boxes at each forecast hour represent the 95% significance interval.

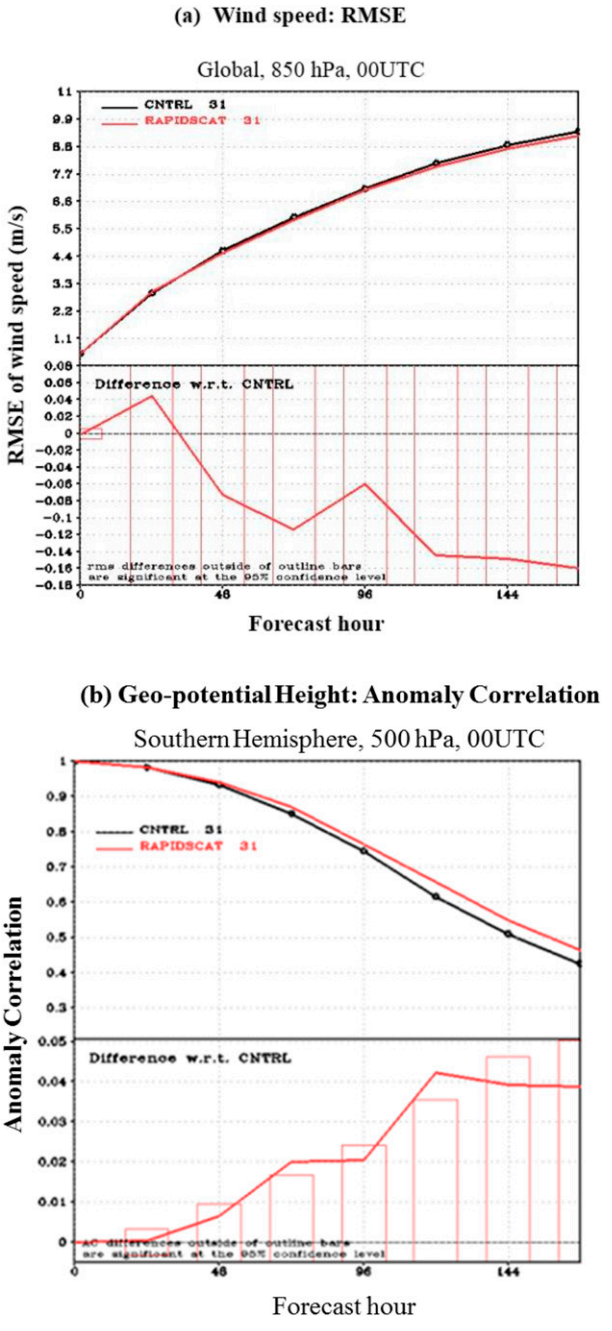

FIG. 12. (a) Global 850-hPa wind RMSE die-off. Red curve in the top panel indicates the forecast impact of new EXRS_nosat experiment and black curve shows the new CNTRL_nosat experiment. The bottom panel indicates the difference of statistics between the EXRS_nosat experiment and the CNTRL_nosat. (b) SH 500-hPa height AC die-off. Red curve in the top panel indicates the forecast impact of new EXRS_nosat experiment and black curve shows the new CNTRL_nosat experiment. The bottom panel indicates the difference of statistics between the EXRS_nosat experiment and the CNTRL_nosat.

EXRS_nosat experiments are switched off, including radiances, GPSRO, ASCAT, and atmospheric motion vectors.

Figure 12 shows that RapidScat has a slightly positive impact on the forecast, especially at longer forecast lead times. Figure 12a shows that globally, RapidScat has a positive, but statistically neutral, impact in 850-hPa wind. However, Fig. 12b shows that the 500-hPa geopotential height anomaly correlation over the Southern Hemisphere has a significant positive impact at days 3 and 5. Over the Northern Hemisphere, the impact on

anomaly correlation is neutral owing to the large volumes of conventional observations assimilated in that region (not shown). Impacts on the wind forecast in the tropics include a statistically significant reduction of RMSE at 200 hPa beyond day 4, but neutral impact on wind at 850 hPa (not shown).

The results of the data denial experiments, therefore, confirm that the impact of RapidScat wind on top of the current global satellite observing system is, indeed, muted, and without those observations, RapidScat, indeed, has a positive impact on the forecast using this version of the NOAA GDAS/GFS.

5. Conclusions

The RapidScat scatterometer deployed on the ISS offers additional observations of surface wind to the global satellite observing system used to characterize the state of the atmosphere and the surface. When stable and operational, RapidScat has offered high-quality observations of surface wind vectors in non-precipitating conditions over data-sparse regions of Earth's oceans. From the preassimilation data quality assessment, quality control procedures are implemented to remove observations flagged as precipitating, as well as observations of wind speeds less than $5\,m\,s^{-1}$. The estimated error of the observations passing quality control, when compared to an independent ECMWF analysis, is approximately $2\,m\,s^{-1}$. Assimilation of the RapidScat wind vector observations passing quality control, with an assumed $2\,m\,s^{-1}$ observation error, shows a slight positive impact on the GDAS surface wind vector analysis when compared to ECMWF analysis. The assimilation of the RapidScat data also has a positive effect on the assimilation of ASCAT surface wind vector observations through improvement of the background field wind vectors, leading to smaller $O - B$ for ASCAT. This demonstrates that RapidScat is providing added information to the data assimilation and forecasts, as well as to the robustness of the global observing system. The GFS forecast impacts, when assessed for the period between 15 June and 31 July 2015, show neutral/nonsignificant impacts for a variety of metrics, including 200-hPa wind, 850-hPa wind, and 500-hPa height, for various regions and forecast hours. Even with the small analysis improvements and neutral forecast improvement, RapidScat adds valuable observations and robustness to the global observing system, which is required for maintaining high forecast skill in medium-range NWP. To confirm this, the second group of experiments assimilated RapidScat wind on top of conventional observations only and indicates that in the absence of other satellite data, RapidScat has a statistically significant positive impact on the forecast. For operational assimilation of RapidScat observations, the unique challenges presented by the ISS platform due to spacecraft maneuvers, their impact on the stability of RapidScat product quality, and the capability of the data assimilation systems to adapt need to be considered.

Acknowledgments. We thank Hurricane Sandy Supplemental Act funding for providing funding support for this study. We also thank the surface wind group from NOAA/NESDIS/STAR for helping us better understand the intrinsics of the wind system. We would also like to thank three anonymous reviewers for their very constructive and helpful suggestions and revision comments. The opinions and findings in this manuscript should not be construed as official NOAA or U.S. government policies or decisions.

REFERENCES

Bi, L., J. A. Jung, M. C. Morgan, and J. F. Le Marshall, 2011: Assessment of assimilating ASCAT surface wind retrievals in the NCEP Global Data Assimilation System. *Mon. Wea. Rev.*, **139**, 3405–3421, https://doi.org/10.1175/2011MWR3391.1.

Chen, S. H., 2007: The impact of assimilating SSM/I and QuikSCAT satellite winds on Hurricane Isidore simulations. *Mon. Wea. Rev.*, **135**, 549–566, https://doi.org/10.1175/MWR3283.1.

Cooley, V. M., 2013: Unique offerings of the ISS as an Earth observing platform. *64th Int. Astronomical Congress*, Beijing, China, International Astronautical Federation, IAC-13-D9.2.8, https://ntrs.nasa.gov/archive/nasa/casi.ntrs.nasa.gov/20140002477.pdf.

Draper, D. W. and D. G. Long, 2002: An assessment of SeaWinds on QuikSCAT wind retrieval. *J. Geophys. Res.*, **107**, 3212, https://doi.org/10.1029/2002JC001330.

Fan, X., J. R. Krieger, J. Zhang, and X. Zhang, 2013: Assimilating QuikSCAT ocean surface winds with the Weather Research and Forecasting Model for surface wind-field simulation over the Chukchi/Beaufort Seas. *Bound.-Layer Meteor.*, **148**, 207–226, https://doi.org/10.1007/s10546-013-9805-2.

Figa-Saldaña, J., J. J. W. Wilson, E. Attema, R. Gelsthorpe, M. R. Drinkwater, and A. Stoffelen, 2002: The advanced scatterometer (ASCAT) on the meteorological operational (MetOp) platform: A follow on for European wind scatterometers. *Can. J. Remote Sens.*, **28**, 404–412, https://doi.org/10.5589/m02-035.

Fore, A. G., B. W. Stiles, A. H. Chau, B. A. Williams, R. S. Dunbar, and E. Rodríguez, 2014: Point-wise wind retrieval and ambiguity removal improvements for the QuikSCAT climatological data set. *IEEE Trans. Geosci. Remote Sens.*, **52**, 51–59, https://doi.org/10.1109/TGRS.2012.2235843.

Gonzales, A. E., and D. G. Long, 1999: An assessment of NSCAT ambiguity removal. *J. Geophys. Res.*, **104**, 11 449–11 457, https://doi.org/10.1029/98JC01943.

Grell, G. A., J. Dudhia, and D. R. Stauffer, 1994: A description of the fifth-generation Penn State/NCAR Mesoscale Model (MM5). NCAR Tech. Note NCAR/TN-398+STR, 122 pp., https://doi.org/10.5065/D60Z716B.

Jones, W. L. and J. Zec, 1996: Evaluation of rain effects on NSCAT wind retrievals. *Proc. Oceans '96: Prospects for the 21st Century*, Fort Lauderdale, FL, Institute of Electrical and Electronics Engineers, 1171–1176, https://doi.org/10.1109/OCEANS.1996.569067.

Madsen, N. M., and D. G. Long, 2016: Calibration and validation of the RapidScat scatterometer using tropical rainforests. *IEEE Trans. Geosci. Remote Sens.*, **54**, 2846–2854, https://doi.org/10.1109/TGRS.2015.2506463.

McClung, T., 2014: Technical implementation notice 14-46. NOAA/NWS Tech. Note. 14-46, http://www.nws.noaa.gov/os/notification/tin14-46gfs_cca.htm.

NASA, 2015: RapidScat reduced power echo anomaly recurrence. NASA/PODAAC, accessed 25 January 2015, https://podaac.jpl.nasa.gov/announcements/2015-10-20_RapidScat_Reduced_Echo_Power_Anomaly_Recurrence.

——, 2016: ISS-RapidScat (ISS RapidScat). NASA, accessed 01 May 2016, http://www.nasa.gov/mission_pages/station/research/experiments/1067.html.

Paget, A. C., D. G. Long, and N. M. Madsen, 2016: RapidScat diurnal cycles over land. *IEEE Trans. Geosci. Remote Sens.*, **54**, 3336–3344, https://doi.org/10.1109/TGRS.2016.2515022.

Rodriguez, E., 2013: The NASA ISS-RapidScat mission. *2013 Fall Meeting*, San Francisco, CA, Amer. Geophys. Union, U23A-03.

Wang, X., D. Parrish, D. Kleist, and J. Whitaker, 2013: GSI 3DVar-based ensemble–variational hybrid data assimilation for NCEP Global Forecast System: Single-resolution experiments. *Mon. Wea. Rev.*, **141**, 4098–4117, https://doi.org/10.1175/MWR-D-12-00141.1.

Yu, T. W., and R. D. McPherson, 1984: Global data assimilation experiments with scatterometer winds from SEASAT-A. *Mon. Wea. Rev.*, **112**, 368–376, https://doi.org/10.1175/1520-0493(1984)112<0368:GDAEWS>2.0.CO;2.